

Exciton spin relaxation in single semiconductor quantum dots

E. Tsitsishvili[*] and R. v. Baltz

Institut für Theorie der Kondensierten Materie, Universität Karlsruhe, D-76128 Karlsruhe, Germany

H. Kalt

Institut für Angewandte Physik, Universität Karlsruhe, D-76128 Karlsruhe, Germany

(Dated: August 9, 2021)

We study the relaxation of the exciton spin (longitudinal relaxation time T_1) in single asymmetrical quantum dots due to an interplay of the short-range exchange interaction and acoustic phonon deformation. The calculated relaxation rates are found to depend strongly on the dot size, magnetic field and temperature. For typical quantum dots and temperatures below 100 K, the zero-magnetic field relaxation times are long compared to the exciton lifetime, yet they are strongly reduced in high magnetic fields. We discuss explicitly quantum dots based on (In,Ga)As and (Cd,Zn)Se semiconductor compounds.

PACS numbers: 78.67.Hc, 72.25.Rb, 63.20.Ls

The current interest in the manipulation of spins in semiconductors is based on the ability to control and maintain spin coherence over practical length and time scales. Of particular interest for possible applications in quantum computing is the storage of spins in zero-dimensional semiconductor structures. Recent theoretical investigations of the single carrier-spin relaxation in semiconductor quantum dots (QDs) found that the electron spin-flip transitions are very slow with relaxation times of milliseconds and longer[1, 2]. But since most concepts for quantum information processing involving QDs are based on optical generation, manipulation and read-out of spins, one has to investigate the dynamics of the excitonic spin. In our previous communication[3] (motivated by experimental results for InAs QDs[4] at high temperatures $T \gtrsim 40$ K), we studied the exciton-spin relaxation in QDs related to a second-order process governed by optical phonons. Further detailed theoretical studies of the exciton-spin relaxation in QDs are still missing.

Experimental investigations on the exciton-spin dynamics in QDs refer mostly to the spin-coherence problem[5, 6, 7] i.e., they determine the transverse relaxation time T_2 . Studies of the longitudinal spin-relaxation time T_1 are rare since they require strict resonant excitation conditions and/or high magnetic fields. Recent resonant-excitation experiments on InAs QDs indicate no exciton-spin relaxation at low temperatures: the exciton-spin is totally frozen during the radiative lifetime even for high magnetic fields up to 8 T[4]. Similar results are reported for CdSe QDs with large lateral dimensions (comparable to twice the exciton Bohr radius of ~ 5 nm in bulk CdSe crystals)[8, 9]. However, longitudinal spin-relaxation times comparable to the exciton lifetime were deduced from high magnetic field experiments for much smaller CdSe QDs[10]. The observed magnetic field dependence (the relaxation rate strongly increases with magnetic fields) points on an acoustic-phonon mediated exciton spin-flip as underlying mechanism. The same conclusion is drawn from the linear temperature

dependence of the spin-relaxation rate reported for non-resonant excitation in InGaAs disks[11].

We propose in this paper an intrinsic mechanism for excitonic spin-flip transitions at low temperatures resulting from a deformation-induced exchange interaction. Our model calculations are able to qualitatively reproduce the above mentioned trends of the experiments. We study the dependence of the exciton spin relaxation time T_1 on temperature, magnetic field, and the QD size. Finally, we draw conclusions on the suitability of various materials for the storage of optically generated spins.

Extensive experimental studies have identified the main features of the exciton fine structure in self-organized QDs by means of single-dot spectroscopy[12, 13]. Such QDs are usually strained and have an asymmetrical shape with a height smaller than the base size. It has been shown that a reduction of the QD symmetry lifts degeneracies among the exciton states and results, in particular, in a splitting of the exciton ground state. Thus, as a consequence of strain and confinement in the growth direction of a QD, the ground states of the heavy-hole (hh) and light-hole (lh) excitons are well-separated and the hh-exciton has the lowest energy. The hh- and lh-exciton quartets are characterized by the projections $J_z = \pm 1, \pm 2$ and $J_z = \pm 1, 0$ of the total angular momenta $J = 1, 2$, respectively. The short-range exchange interaction splits the ground states of both hh- and lh-excitons into doublet states (so-called singlet-triplet splitting), as is shown in Fig. 1(a). The lateral anisotropy of a QD leads to a further splitting of the optically allowed doublets $|\pm 1\rangle$ into two levels (labeled $|X\rangle$ and $|Y\rangle$) with dipole moments along the two nonequivalent in-plane QD axes. This splitting is due mostly to the long-range exchange interaction and originates from the lateral elongation of the QD's[12, 14, 15]. Continuous wave single-dot spectroscopy experiments have clearly evidenced the two related, linearly polarized optical transitions e.g., in GaAs interfacial dots [16] or self-organized InGaAs QD's[13]. Measured magnitudes of this splitting reach some tens or even hundreds of μeV [4, 13, 16]. Re-

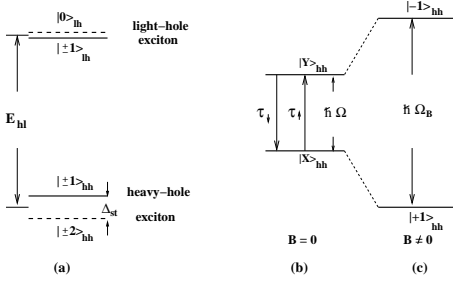


FIG. 1: Schematic diagram showing (a) the sublevels of the heavy-hole-exciton and light-hole-exciton ground states in symmetrical QDs, (b) the phonon-assisted spin-flip processes within the radiative doublet of the heavy-hole-exciton in an asymmetrical QD, and (c) the Zeeman radiative doublet of the heavy-hole-exciton. Optically inactive states are shown by dashed lines.

laxation processes between the radiative states changes the occupation of the exciton levels and are manifested in a change of the linear degree of polarization of the luminescence[3, 4].

In what follows we consider (longitudinal) spin-relaxation processes between the allowed $|X\rangle$ - and $|Y\rangle$ -states of the hh-exciton. In such processes, the hh-exciton stays in the same spatial state and just flips its spin (i.e., the electron and the hole spin flip simultaneously), by emitting or absorbing an acoustic phonon. Since the bare electron/hole-phonon interaction does not contain spin operators, it cannot directly couple the involved exciton states, however, this can occur via the hh and lh exciton mixing due to the interplay of the the short-range exchange interaction and the lattice deformations.

The short-range (isotropic) exchange interaction is given by the Hamiltonian [17]

$$\mathcal{H}_{ex} = -\frac{2}{3} \Delta_{st} \vec{\sigma} \vec{J}, \quad (1)$$

where $\vec{\sigma}$ and \vec{J} are the electron spin and the hole total angular momentum operator, respectively, and Δ_{st} is the (singlet-triplet) exchange energy. Phonon-induced deformations come into play via the off-diagonal terms in the Bir-Pikus Hamiltonian[17]

$$\mathcal{H}(\varepsilon) = b \sum_i J_i^2 \left(\varepsilon_{ii} - \frac{1}{3} \varepsilon \right) + \frac{2}{\sqrt{3}} d \sum_{i>j} [J_i J_j] \varepsilon_{ij}, \quad (2)$$

where b and d are the exciton deformation potentials, ε_{ij} is the deformation tensor, and $[J_i J_j] = J_i J_j + J_j J_i$. (An overall shift of $-a\varepsilon$ of the lh and hh exciton levels is omitted).

In the basis of the hh- and lh-exciton states ($| - 1 \rangle_{hh}$, $| + 1 \rangle_{hh}$ and $| - 1 \rangle_{lh}$, $| + 1 \rangle_{lh}$, respectively), the total Hamiltonian $\mathcal{H} = \mathcal{H}(\varepsilon) + \mathcal{H}_{ex}$ is represented by the following

matrix

$$\mathcal{H} = \begin{vmatrix} 0 & 0 & \frac{\Delta_{st}}{\sqrt{3}} & j^* \\ 0 & 0 & j & \frac{\Delta_{st}}{\sqrt{3}} \\ \frac{\Delta_{st}}{\sqrt{3}} & j^* & E_{lh} & 0 \\ j & \frac{\Delta_{st}}{\sqrt{3}} & 0 & E_{lh} \end{vmatrix}. \quad (3)$$

The origin of energy axis is fixed at the hh-exciton states which are separated from the lh-exciton by E_{lh} , see Fig. 1(a). The deformation-dependent off-diagonal term is $j = \sqrt{3}b(\varepsilon_{xx} - \varepsilon_{yy})/2 - id\varepsilon_{xy}$. Here, we neglect the anisotropic part of the splitting of the allowed doublets, since the energy difference E_{lh} is, typically, much larger (of the order of several tens of a meV) than the fine structure energies[12]. For the same reason, the hh-lh-exciton mixing can safely be regarded as a perturbation. It follows from Eq. (3) that perturbations which mix hh- and lh-exciton states result in a coupling of the $| - 1 \rangle_{hh}$ - and $| + 1 \rangle_{hh}$ -states and, consequently, lead to the mixing of the $|X\rangle$ - and $|Y\rangle$ -states of the hh-exciton. For QDs which are elongated in the $[110]$ direction, this coupling is due to vibrations causing $(\varepsilon_{xx} - \varepsilon_{yy})$ deformations

$$\langle X | \mathcal{H} | Y \rangle = -i \frac{(j + j^*) \Delta_{st}}{\sqrt{3} E_{lh}} \equiv -i \frac{\Delta_{st}}{E_{lh}} b (\varepsilon_{xx} - \varepsilon_{yy}). \quad (4)$$

Thus, a coupling of the $|X\rangle$ - and $|Y\rangle$ -states is a result of an interplay between the short-range exchange interaction and deformations: neither the exchange interaction nor the deformation perturbation j alone can couple these states. According to Eq. (4), the matrix element for the relaxation processes among the $|X\rangle$ - and $|Y\rangle$ -states of the hh-exciton is

$$M_{XY} = -i \frac{\Delta_{st}}{E_{lh}} b \langle (\varepsilon_{xx} - \varepsilon_{yy}) \rangle, \quad (5)$$

where the expectation value is taken with respect to the spatial part of the exciton wave function. The elastic strain is given by

$$\varepsilon_{ij} = \frac{1}{2} \left(\frac{\partial u_i}{\partial r_j} + \frac{\partial u_j}{\partial r_i} \right), \quad (6)$$

where the phonon displacement field is

$$\vec{u} = \frac{1}{\sqrt{V}} \vec{e}(\vec{q}) \sqrt{\frac{\hbar}{2\rho\omega_q}} \left(e^{i\vec{q}\vec{r}} a_{\vec{q}} + e^{-i\vec{q}\vec{r}} a_{\vec{q}}^{\dagger} \right). \quad (7)$$

Here \vec{q} , \vec{e} and $\omega_q = sq$ are the phonon momentum ($q = |\vec{q}|$), polarization vector and frequency, respectively, V is the normalization volume, ρ is the mass density, and s is the sound velocity. Upon substitutions given by Eqs. (6) and (7) we obtain for the matrix element in Eq. (5)

$$|M_{XY}|^2 = \frac{1}{V} \left(\frac{\Delta_{st}}{E_{lh}} \right)^2 \frac{\hbar b^2}{2\rho\omega_q} (q_x e_x - q_y e_y)^2 |M_{or}|^2, \quad (8)$$

$$M_{or}(\vec{q}) = \langle \Phi_0 | e^{i\vec{q}\vec{r}_e} + e^{i\vec{q}\vec{r}_h} | \Phi_0 \rangle, \quad (9)$$

where indices e and h stand for electrons and holes, M_{or} is the orbital part of the matrix element, and $\Phi_0(\vec{r}_e, \vec{r}_h)$ is the exciton ground state envelope wave function.

The spin-relaxation rates accompanied by phonon emission and absorption are given by Fermi's golden rule

$$\begin{aligned} \frac{1}{\tau_{\downarrow}} &= \frac{2\pi}{\hbar} \sum_{\vec{q}} \sum_{\vec{e}} |M_{XY}|^2 \delta(\hbar\Omega - \hbar\omega_q) (N_{\omega_q} + 1), \\ \frac{1}{\tau_{\uparrow}} &= \frac{2\pi}{\hbar} \sum_{\vec{q}} \sum_{\vec{e}} |M_{XY}|^2 \delta(\hbar\Omega - \hbar\omega_q) N_{\omega_q}, \end{aligned} \quad (10)$$

where $\hbar\Omega$ is the energy splitting between the $|X\rangle^-$ and $|Y\rangle^-$ -states (see Fig. 1(b)), and $N_{\omega_q} = 1/(e^{\hbar\omega_q/k_B T} - 1)$ is the thermal phonon distribution function.

We discuss now what determines the value of the orbital part of the matrix element Eq. (9). Because of energy conservation, $|M_{or}| \equiv |M_{or}^e + M_{or}^h|$ has to be calculated for the phonon momentum $q = \omega_q/s \equiv \Omega/s$, while the characteristic extent of the orbital wave function Φ_0 is, roughly speaking, the lateral size L of the QD. (For flat QDs, the QD height $L_z \ll L$.) Due to the oscillatory behavior of the exponential functions in M_{or} , we have $|M_{or}^{e,h}| \approx 1$, if $\Omega L/s \lesssim 1$. To illustrate this approximation, we consider the model of a strongly confined QD with the shape of a parallelepiped and infinite barrier. Then the exciton states are reasonably well approximated by noninteracting electron-hole pair states. In addition, the single carrier-phonon matrix element $|M_{or}^e(\vec{q})| = |M_{or}^h(\vec{q})| \equiv |M_{or}(\vec{q})|$ separates in the x, y, z coordinates. For a confined direction (say, the x -direction), the following expression holds

$$|M_{or}(q_x)| = \left| \frac{\sin Q_x}{Q_x} + \frac{Q_x \sin Q_x}{Q_x^2 - \pi^2} \right|, \quad (11)$$

where $Q_x = q_x L_x/2$ and L_x is the QD size in the x -direction. As seen from Eq. (11), the matrix element $|M_{or}(q_x)|$ is smaller than unity for any $q_x \neq 0$, but it approaches unity for small $q_x L_x \ll 1$ ($|M_{or}(q_x)| \sim |1 - Q_x^2/\pi^2|$). With increasing $q_x L_x \gg 1$, $|M_{or}(q_x)|$ decreases rapidly ($|M_{or}(q_x)| \sim |\sin Q_x/Q_x|$). Thus, if we replace the orbital matrix element in Eq. (8) by unity, $|M_{or}(\vec{q})|^2 \equiv 1$, the exciton-spin relaxation rates Eq. (10) will be overestimated. Note that for typical values of Ω and s we have $(s/\Omega) \sim 40$ nm, L is usually about 10-20 nm[18], so that the above mentioned assumption $\Omega L/s \lesssim 1$ is reasonable. As a result, a lower limit for the relaxation times is given by

$$\begin{aligned} \tau_{\downarrow} &= \frac{9}{4} \frac{\hbar\rho s^2}{b^2} \left(\frac{E_{lh}}{\Delta_{st}} \right)^2 \left(\frac{s}{\Omega} \right)^3 \left(1 - e^{-\hbar\Omega/k_B T} \right), \quad (12) \\ \tau_{\uparrow} &= \tau_{\downarrow} e^{\hbar\Omega/k_B T}. \quad (13) \end{aligned}$$

In order to obtain a numerical estimate, we use typical parameters[18], together with an estimated hh-lh-exciton splitting of $E_{lh} = 10$ meV, i.e., $E_{lh}/\Delta_{st} = 50$. As a result, we get for the spin relaxation time scale $T_1 \equiv (\tau_{\downarrow}^{-1} + \tau_{\uparrow}^{-1})^{-1} \sim 1500$ ns (at $T = 10$ K) and $T_1 \sim 150$ ns

(at $T = 100$ K). Thus, for typical quantum dots and low temperatures, the zero-magnetic field relaxation times are very long compared to the exciton lifetimes of ~ 1 ns. This is in qualitative agreement with resonant-excitation experiments at low temperatures[4, 8]. Please note, that because of the small interlevel splitting $\hbar\Omega \sim 0.1$ meV, the relaxation times τ_{\downarrow} and τ_{\uparrow} are already comparable at $T \gtrsim 2$ K. For higher temperatures T_1 is inversely proportional to the temperature. But for $T \gtrsim 100$ K, the interaction with LO phonons via a second-order process will be the dominant relaxation mechanism[3, 4].

The calculated spin relaxation times according to Eqs. (12,13) are large partly because of the small phonon density of the states (which is $\sim (\Omega/s)^2$) at the scale of the interlevel splitting $\hbar\Omega$. But, considerably large interlevel splittings of $\hbar\Omega_B = g\mu_B B \sim 1.5$ meV (where g is the exciton effective g -factor) arise in high-field magneto-optical experiments. Here an enhancement of spin-relaxation rate is expected. The spin flip in Faraday geometry ($\vec{B} \parallel z$) occurs between the $|-1\rangle_{hh}$ - and $|+1\rangle_{hh}$ - states of the hh-exciton (see Fig. 1(c))[12]. Consequently, exciton-spin relaxation processes between the Zeeman sublevels are reflected in a change of the circular degree of polarization of the luminescence.

For magnetic fields and zero temperature, a lower limit of the spin relaxation time is given by

$$T_1(B) \simeq \tau_{\downarrow}(B) = \frac{9}{4} \frac{\hbar\rho s^2}{b^2} \left(\frac{E_{lh}}{\Delta_{st}} \right)^2 \left(\frac{s}{\Omega_B} \right)^3, \quad (14)$$

$$\tilde{b}^2 = b^2 + \frac{\Omega_B}{3\sqrt{\Omega_B^2 + 4\Omega^2}} d^2, \quad (15)$$

$$\tilde{\Omega}_B = \Omega + \Omega_B. \quad (16)$$

The relaxation time in Eq. (16) varies as the square of the ratio E_{lh}/Δ_{st} and depends strongly on the QD size because both the splitting E_{lh} and the exchange energy Δ_{st} are size-dependent[20, 21]. If the splitting E_{lh} is due mostly to the strain (large lattice mismatch), T_1 changes with the lateral and vertical size as L^4 and L_z^2 , respectively. For small lattice mismatch, E_{lh} is due mostly to the vertical confinement and, therefore, $T_1 \sim L^4 L_z^{-2}$. In any case, the relaxation time T_1 strongly decreases when decreasing the lateral size L of a QD. This result can explain qualitatively the observations for the CdSe QDs of different lateral sizes in high magnetic fields. As noted above, no spin relaxation was found for large CdSe QDs (with L about 10 nm)[9], while for small CdSe QDs (with L about 3 nm - 5 nm) an efficient exciton-spin relaxation was observed [10].

To obtain numerical estimates for the spin relaxation in magnetic fields, we use the experimental values for E_{lh} , Δ_{st} and g , and we take the typical values[18] for other factors in Eq. (14). For InAs/GaAs QDs, we use $\Delta_{st} = 0.2$ meV, $g = 3$ [13] and $E_{lh} = 30$ meV (E_{lh} of several tens of a meV is reported in Ref.[12]). As a result we get a lower limit for the relaxation time $T_1 \simeq 13/B^3$ ($\mu\text{s T}^3$) which is much larger than the exciton lifetime scale ~ 1 ns even at high B (e.g., $T_1 \simeq 25$ ns at $B = 8$ T).

Indeed, no spin relaxation is found for low temperature experiments in high magnetic fields [4].

This case is different for small CdSe/ZnSe QDs investigated in Ref.[10, 22]. Here, values of $\Delta_{st} \sim 1$ meV, $g \sim 2$ and $E_{lh} \sim 40$ meV are reported. As a result we calculate $T_1 \sim 5$ ns at $B = 6$ T which is close to values of 2.5 ns - 3.4 ns deduced from the experiments[10]. For large CdSe/ZnSe QDs investigated in Ref.[9] no data on the exchange energy Δ_{st} are reported but we still can estimate the relaxation rate. The lateral size of the QDs in this case is about a factor of 2.5 larger than in [10]. The consequence is a much smaller exchange splitting $\Delta_{st} \sim 0.2$ meV [21] which results in much longer relaxation times of ~ 100 ns (at $B = 6$ T). As already mentioned, no spin relaxation is observed in the experiments of Ref.[9].

Let us now consider the magnetic field dependence of the spin-relaxation time which was measured in small CdSe/ZnSe QDs [10]. The experimental results indicate a roughly anti-proportional decrease $T_1 \propto B^{-1}$ up to 8 T. As seen from Eqs. (14,16), T_1 scales as B^{-1} for small B ($\Omega_B < \Omega$), in agreement with the experiment. But it would depend much stronger on the magnetic field (as B^{-3}) for large B . This difference to the experiment can originate from the treatment of the orbital matrix element, which up to now has been fixed as 1. But a factor of $1/|M_{or}|^2$ has to be accounted for explicitly in Eq. (14) for high magnetic fields. The reason is, that the relevant phonon momentum $q(B) \simeq \Omega_B/s$ is linearly proportional to B . Thus, $1/|M_{or}|^2$ increases with magnetic field and becomes important at $q(B)L \geq 1$. This is the case e.g., for $B > 5$ T for CdSe QDs with a lateral size of $L \sim 4$ nm and is the regime of the experiments in [10]. So we can confirm the general trend of the experiment[10], namely that T_1 decreases with magnetic field. An analytical dependence of T_1 on B (at high B) would require an explicit calculation of $|M_{or}|^2$ with the QD exact parameters, which for the QDs used in Ref.[10], unfortunately, are not known.

There are many experiments, which determine the polarization degree of the luminescence from QDs under nonresonant excitation conditions. We just want to discuss the results of Ref.[11] as a typical representative. Rather short polarization decay times on the order of 1 ns have been found here. But definite conclusions on the underlying spin-relaxation mechanisms are not possible in a scenario where the electron-hole pairs relax through a multitude of barrier states and/or excited quantum-dot states. To identify spin-relaxation processes, the splitting of the exciton ground state has to be large (as for large magnetic fields) or strictly resonant excitation has to be used (see [4]).

The above discussions show that a direct quantitative comparison of our proposed relaxation model to experimental data is at the moment difficult at best. One obvious reason is that the relaxation times, once they are much larger than the exciton lifetime, cannot be quantified experimentally. The second reason is, that only very few experiments under strict resonant excita-

tion and/or in high magnetic fields have been performed. But still, there are a couple of experimental trends which are explained consistently by our model. The value and magnetic-field dependence of T_1 in small CdSe QDs can be reproduced. We correctly predict the experimental findings that long relaxation times are expected for InAs QDs as well as large CdSe QDs at low temperatures even in strong magnetic fields.

The experimental differences found for InAs vs CdSe QDs and for large vs small CdSe QDs strongly support our proposed model. Let's consider alternative spin-relaxation mechanisms within the radiative doublet. Processes relying on the exciton motion like for quantum-well excitons [23] are suppressed in QDs. Assume, the electron and hole would individually flip their spins. In contrast to our proposed mechanism, this is a higher-order process involving intermediate dark exciton states (the excitons finally have to return to radiative states to contribute to a depolarized luminescence). The relaxation time here is determined by the longest spin-flip time for a single carrier (electron or hole). The spin flip of the electron has to rely on mechanisms based on the spin-orbit coupling. These relativistic effects have been shown by Khaetskii and Nazarov [1] to be inefficient in QDs. Finally, the spin-orbit interaction and carrier-phonon coupling are not different enough in InAs and CdSe or for large and small QDs to explain that the spin relaxation times change by orders of magnitude. This dramatic change found in the experiments is, however, readily explained by the strongly differing exchange splitting in InAs and CdSe and its significant enhancement in small dots. Since the exchange splitting enters quadratically in our proposed relaxation scheme, we are quite convinced to have identified the most prominent spin-relaxation process for QDs.

Finally, we want to discuss different material systems with respect to their suitability for spin storage. The relevant parameters for several semiconductor compounds forming QD's and their matrices are presented in Table I. Among the different material parameters in Eq. (16), the characteristic energies E_{lh} and Δ_{st} are strongly affected by the structural composition. Thus we can only give general trends. We will consider QDs with typical sizes of about $L_z \sim 2-5$ nm and $L \sim 10-20$ nm which are in the strong vertical confinement regime. Moreover, $\text{In}_x\text{Ga}_{1-x}\text{As}$ QDs are also strongly confined in the lateral plane, and the exchange splitting Δ_{st} in these QDs significantly exceeds its bulk value of Δ_{st}^b [21]. In CdSe QDs the bulk value of the exchange splitting is already quite large. In CdSe QDs with lateral sizes larger than the exciton radius of $a_{ex} \sim 5$ nm the exchange splitting is additionally affected by the vertical confinement. Since the exchange interaction in (In,Ga)As crystals is much weaker than in CdSe crystals, Δ_{st} is of the same order of magnitude[24] in strongly confined $\text{In}_x\text{Ga}_{1-x}\text{As}$ QDs and large, weakly confined CdSe QDs. Considering additionally the strain-induced lh-hh splitting E_{lh} , which has to be large to suppress spin relaxation, InAs QDs have the

TABLE I: Semiconductor compounds forming QDs (first column) and matrices (sixth column), Δ_{st}^b and a_{ex} are the exchange splitting and the exciton Bohr radius in bulk compounds forming QDs, Δ_{st} gives typical values of the exchange splitting in QDs with sizes of $L_z = 3$ nm and $L = 15$ nm. $m_0/m = m_0(1/m_{lh} - 1/m_{hh})$, where m_{lh} and m_{hh} are the lh- and hh-masses, respectively. $|\Delta a|/a = (a_d - a_m)/0.5(a_d + a_m)$ and $\Delta E_g = E_{gm} - E_{gd}$ with lattice constants a_d and a_m and energy gaps E_{gd} and E_{gm} in the QD and matrix materials, respectively. Material constants are taken from Ref. 19, except Δ_{st}^b and a_{ex} for InAs crystals which are taken from Ref. 25. For the case of CdSe crystals, Δ_{st}^b , a_{ex} , ΔE_g , and m_0/m are given for hexagonal CdSe crystals.

QD	a_{ex} (nm)	Δ_{st}^b (μeV)	Δ_{st} (μeV)	$\frac{m_0}{m}$	matrix	$\frac{ \Delta a }{a}$	ΔE_g (eV)
InAs	38	0.3	200	37.5	GaAs	0.069	1.1
InAs	38	0.3	200	37.5	Al _{0.3} Ga _{0.7} As	0.068	1.8
GaAs	11	20	250	9.3	Al _{0.3} Ga _{0.7} As	0.0005	0.48
In _{0.6} Ga _{0.4} As	24	8.2	220	17.7	GaAs	0.042	0.62
In _{0.4} Ga _{0.6} As	22	12.1	230	13.8	Al _{0.5} Ga _{0.5} As	0.027	1.22
In _{0.7} Ga _{0.3} As	31	6.2	210	20.6	GaAs	0.049	0.73
CdSe	5.4	130	450	4.7	ZnSe	0.066	0.9

longest relaxation time T_1 .

Less suitable for spin storage is the GaAs/Al_{0.3}Ga_{0.7}As system since its lattice mismatch is very small. Thus, among the QD structures listed in Table I, the shortest T_1 relaxation times can be expected for strongly confined GaAs/Al_{0.3}Ga_{0.7}As QDs. Likewise, small T_1 times are predicted for small CdSe QDs since in the strong lateral confinement regime, Δ_{st} is considerably enhanced.

In conclusion, the exciton–spin relaxation within the radiative doublet of the exciton ground state in single asymmetrical QDs is studied. As a possible intrinsic mechanism for such a process, the exciton spin–acoustic phonon coupling via the strain–dependent short range exchange interaction is proposed. For zero-magnetic fields and low temperatures, the calculated T_1 –relaxation times for typical QDs are long compared to the exciton lifetime. A strong reduction of the relaxation times occurs

in QDs in high magnetic fields. Nevertheless, numerical estimates for InAs QD’s and large CdSe QDs give large values for the T_1 –relaxation times even for high $B \sim 8$ T (up to a few of tens of nanoseconds). In addition, the relaxation time T_1 strongly decreases in strongly confined (in the lateral plane) QDs. The T_1 –relaxation times estimated for small CdSe QDs in high magnetic fields reduce to the nanosecond scales. These predictions of our model are in qualitative agreement with experimental findings. Within the considered mechanism, we conclude that InAs QDs and CdSe QDs with typical lateral sizes of $L \sim 10 - 20$ nm display a weak exciton spin relaxation, whereas for typical GaAs/Al_{0.3}Ga_{0.7}As QDs and small CdSe QDs the T_1 times are expected to be rather short.

This work was supported by the Center for Functional Nanostructures (CFN) of the Deutsche Forschungsgemeinschaft (DFG) within project A2.

[*] Permanent address: Institute for Cybernetics, Academy of Science, S. Euli 5, 380086, Georgian Republic.

[1] Alexander V. Khaetskii and Yuli V. Nazarov, Phys. Rev. B **64**, 125316 (2001).
[2] L.M. Woods, T.L. Reinecke, and Y. Lyanda-Geller, Phys. Rev. B **66**, 161318(R) (2002).
[3] E. Tsitsishvili, R. v. Baltz, and H. Kalt, Phys. Rev. B **66**, 161405(R) (2002).
[4] M. Paillard, X. Marie, P. Renucci, T. Amand, A. Jbeli, and J.M. Gerard, Phys. Rev. Lett. **86**, 1634 (2001) and references cited therein.
[5] J.A. Gupta, D.D. Awschalom, X. Peng, and A.P. Alivisatos, Phys. Rev. B **59**, R10421 (1999).
[6] P. Borri, W. Langbein, S. Schneider, U. Woggon, R.L. Sellin, D. Ouyang, and D. Bimberg, Phys. Rev. Lett. **87**, 157401 (2001).
[7] D. Birkedal, K. Leosson, and J.M. Hvam, Phys. Rev. Lett. **87**, 227401 (2001).

[8] T. Flissikowski, A. Hundt, M. Lowisch, M. Rabe, and F. Henneberger, Phys. Rev. Lett. **86**, 3172 (2001).
[9] A. Hundt, T. Flissikowski, M. Lowisch, M. Rabe, and F. Henneberger, Phys. Status Solidi B **224**, 159 (2001).
[10] Y. Oka, S. Permogorov, R. Pittini, J.X. Shen, K. Kayanuma, A. Reznitsky, L. Tennishev, and S. Verbin, Physica E **10**, 315 (2001).
[11] H. Gotoh, H. Ando, H. Jamada, A. Chavez-Pirson, and J. Temmyo, Appl.Phys.Lett. **72**, 1341 (1998).
[12] For recent review see M. Bayer, G. Ortner, O. Stern, A. Kuther, A.A. Gorbunov, A. Forchel, P. Hawrylak, S. Fafard, K. Hinzer, T.L. Reinecke, S.N. Walck, J.P. Reithmaier, F. Klopff, and F. Schäfer, Phys. Rev. B **65**, 195315 (2002).
[13] M. Bayer, A. Kuther, A. Forchel, A. Gorbunov, V.B. Timofeev, F. Schäfer, J.P. Reithmaier, T.L. Reinecke, and S.N. Walck, Phys. Rev. Lett. **82**, 1748 (1999).
[14] E.L. Ivchenko, Phys. Status Solidi A **164**, 487 (1997) and

references cited therein.

- [15] E.L. Ivchenko and G.E. Pikus, *Superlattices and Other Heterostructures. Symmetry and Optical Phenomena* (Springer-Verlag, Berlin, 1995).
- [16] D. Gammon, E. S. Snow, B. V. Shanabrook, D. S. Katzer, and D. Park, Phys. Rev. Lett. **76**, 3005 (1996).
- [17] G.L. Bir and G.E. Pikus, *Symmetry and Strain-Induced Effects in Semiconductors* (Wiley, New York, 1975).
- [18] Typical fine structure energies are: $\hbar\Omega \simeq 0.1\text{meV}$, $\Delta_{st} = 0.2\text{meV}$. [12] Typical material parameters are: $s = 5 \times 10^5\text{ cm/sec}$, $\rho = 5.3\text{g/cm}^3$, $b = 2\text{ eV}$, $d = 5\text{ eV}$. [19]
- [19] Landolt-Börnstein, in *New Series*, edited by O. Madelung, M. Schultz, and H. Weiss, (Springer-Verlag, Berlin, 1982), Vol. 17b, Group III.
- [20] T. Takagahara, Phys. Rev. B **47**, 4569 (1993).
- [21] The exchange splitting in strongly confined QD's can be estimated as $\Delta_{st} \sim \Delta_{st}^b a_{ex}^3 / R_z R^2$, where $R_z = L_z/2$ and $R = L/2$.
- [22] S. Verbin, O.Z. Karimov, A. Reznitsky, A.A. Klochikhin, T. Ruf, L. Tenishev, S. Permogorov, S.V. Ivanov, D. Wolverson, and J.J. Davies, Phys. Status Solidi B **224**, 545 (2001).
- [23] M.Z. Maialle, E.A.de Andrada e Silva, and L.J. Sham, Phys. Rev. B **47**, 15776 (1993).
- [24] The exchange interaction for excitons and atoms differs approximately by a factor of (a^3/a_{ex}^3) [17] (where a is the lattice constant), which results in the similar values of a quantity $\Delta_{st}^b a_{ex}^3 \sim 2 \times 10^4 \mu\text{eV nm}^3$ for different materials. Consequently, Δ_{st} are close in QD's of different composition but equal sizes. For the case of $R > a_{ex}$, $\Delta_{st} \sim \Delta_{st}^b a_{ex} / R_z$.
- [25] Huaxiang Fu, Lin-Wang Wang, and Alex Zunger, Phys. Rev. B **59**, 5568 (1999).